INORGANIC CHEMISTRY
FRONTIERS

CHINESE CHEMICAL SOCIETY

ROYAL SOCIETY OF CHEMISTRY

RESEARCH ARTICLE

View Article Online
View Journal | View Issue

Check for updates

Cite this: *Inorg. Chem. Front.*, 2024, **11**, 3458

Received 2nd April 2024,
Accepted 4th May 2024

DOI: 10.1039/d4qi00831f

rsc.li/frontiers-inorganic

Fullerene rotation dictated by benzene–fullerene interactions†

Yaofeng Wang[b] and Fupin Liu *[a,b]

The movement of metal ions inside the fullerene cage signifies the unique structural character of metallofullerenes; however, concrete details on this movement are extremely difficult to observe. In this work, we elucidated the structure of $Dy_2ScN@C_{80}$ using variable temperature single crystal X-ray diffraction. Dynamic disorders with the Dy_2ScN and C_{80} rotations driven by temperature were precisely presented in detail. The position of the solvent molecule benzene in the crystal lattice proved to have a powerful impact on hindering fullerene rotation. These results present a deep understanding of the unique structural character of metallofullerenes, facilitating their high-accuracy structure–property relationship investigation.

The fullerene cage provides a robust confining arena for metal clusters that are otherwise unstable, allowing for the investigation of their peculiar structures/interactions and interesting properties. Versatile metal clusters have been discovered to be hosted by fullerene cages, and these fullerenes show application potential in biomedicine and materials science.[1–4] Elucidating the structures of these metallofullerenes with single-crystal X-ray diffraction proved powerful in understanding these novel molecules.[5–14] Determining the structure with high accuracy is fundamentally important to understand their properties such as bonding interactions between the entities of metallofullerenes and the crystal field around the metal ions.[15–23] The ubiquitous disorders (more than 95%) in metallofullerene crystals originate from the round shape of fullerene cages, which tend to rotate in the crystal lattice, and the shallow potential energy surface supplied by the fullerene cage to hold the encapsulated metal ions.[24–26] Co-crystallization with metal octaethylporphyrin or decapyrrylcorannulene significantly constrained the rotation of fullerene cages.[27,28] However, the rotation of metal clusters in the fullerene cages persists as its intrinsic character.[24–26,29,30] Trimetallic nitride clusterfullerenes have attracted broad interest since their discovery.[6,31] A diversified combination of the metal ions from transition and rare-earth metals produces molecules with fascinating single-molecule magnetism represented by $DyM_2N@C_{80}$ and $Dy_2MN@C_{80}$ (M = Sc,[32–36] Y,[37,38] La,[38] ErSc,[39] Lu,[40] or V[41]).[42] The combination of cluster rotation with mixed metals presents a great challenge in their structural elucidation by single crystal X-ray diffraction because the overlapping between different metal ions precludes their accurate assignment.[33,38,39,43] Recently, we observed the snapshots of M_3N rotation inside the C_{80} cage with spinning top character for heavy metal ions (Ho and Lu),[26] while strong rotation for light metal ions (Sc).[24] Interestingly, the C_{80} cage rotation in these crystals was blocked up to 280 K. On the other hand, it is notable that $Sc_3N@C_{70}$ shows fullerene cage rotation starting from 160 K.[25] Since the symmetry of C_{70} (C_{2v}) is lower than that of C_{80} (I_h), it is expected that C_{80} has a lower energy barrier for rotation, thus requiring a lower temperature to drive its rotation in the same environment. The driving force for fullerene cage rotation in the crystal lattice is fascinating and still unclear. Herein, we precisely determined the structure of $Dy_2ScN@C_{80}$ using variable temperature single crystal X-ray diffraction. The C_{80} cage and Dy_2ScN cluster rotations driven by temperature were precisely recorded with great details. Surprising effects of solvent benzene–fullerene interactions on the fullerene rotations were disclosed, revealing the subtle driving force for fullerene cage rotation in the crystal lattice.

Single crystals were obtained by co-crystallization of $Dy_2ScN@C_{80}$ in benzene with nickel octaethylporphyrin (NiOEP) in benzene through solvent diffusion/evaporation. X-ray diffraction data collection was carried out at the BESSY storage ring (BL14.2, Berlin-Adlershof, Germany).[44] The XDSAPP2.0 suite was employed for data processing.[45,46] The structures were solved using direct methods and refined using SHELXL-2018.[47] Hydrogen atoms were added geometrically and refined with a riding model. The crystal data are presented

---

[a] *Jiangsu Key Laboratory of New Power Batteries, School of Chemistry and Materials Science, Nanjing Normal University, Nanjing 210023, China.*
E-mail: liu_fupin@nnu.edu.cn
[b] *Leibniz Institute for Solid State and Materials Research (IFW Dresden), Helmholtzstr. 20, 01069 Dresden, Germany*

† Electronic supplementary information (ESI) available. CCDC 2330927–2330929. For ESI and crystallographic data in CIF or other electronic format see DOI: **https://doi.org/10.1039/d4qi00831f**

in Table S1 in the ESI.† The asymmetric unit contains one intact NiOEP, one intact fullerene, one intact benzene, and two halves of benzene. The fullerene cage (fully ordered $I_h(7)$-C_{80} at 100 K, (symmetry notation $I_h(7)$ will be omitted hereafter)) sits onto the NiOEP as shown in Fig. 1. The packing characteristics show the typical packing character of fullerene–NiOEP co-crystals, in which one fullerene molecule is supported by one NiOEP, as shown in the $DySc_2N@C_{80}$-NiOEP co-crystals.[32]

The encapsulated Dy_2ScN cluster presents a slight disorder in the structure obtained at 100 K as shown in Fig. 1 and Fig. S1 in the ESI.† Three sites were refined with a site occupancy ratio of 0.67 : 0.29 : 0.04 for Dy_2Sc. The significant size differences of Dy and Sc in the round C_{80} cage push the N out of the C_{80} centroid (*vide infra*); a similar disorder of N with three positions accordingly should be present along with the disordered Dy_2Sc cluster. However, because of the rather short distances between the possible positions and the large differences of the site occupancies, it is difficult to refine all these positions accurately. Two N sites were refined with a site occupancy ratio of 0.81 : 0.19. The structure of Dy_2ScN is evaluated with the main position Dy_2ScN, which shows M–N bond lengths of 1.95(2), 2.07(2), and 2.079(5) Å, and bond angles of ∠Dy1N1ADy2 = 120.8(5)°, ∠Dy1N1ASc1 = 122.9(6)°, and ∠Dy2N1ASc1 = 116.3(3)°, indicating a planar Dy_2ScN cluster. The N was pushed out of the centroid of C_{80} by the asymmetrical Dy_2Sc cluster by 0.19(1) Å. The Dy ion far away from NiOEP is located under a hexagon/pentagon with a Dy–hexagon distance of 2.0095(6) Å (Dy–C bond lengths range from 2.345(4) to 2.599(4) Å), while the other Dy ion is located under a hexagon with a Dy–hexagon distance of 1.9670(5) Å (Dy–C bond lengths range from 2.433(4) to 2.464(4) Å). The Sc ion is located under a hexagon/pentagon with a Sc–hexagon distance of 1.851(8) Å (Sc–C bond lengths range from 2.238(7) to 2.492(7) Å). For comparison, the Dy–hexagon distance of $DySc_2N@C_{80}$ is 2.0241(8) Å, while the Dy–N and Sc–N bond lengths are 2.096 (6), 1.965(6), and 1.978(6) Å,[32] showing noticeable compression of Dy_2ScN by the C_{80} cage.

Variable temperature single crystal X-ray diffraction was used to observe the detailed metal movement in the fullerene cage. In striking contrast to the previous reports on analogous $M_3N@C_{80}$ (M_3 = Ho_2Lu, Lu_3, Sc_3) without fullerene cage rotation until 280 K,[24,26] the fullerene cage here presents rotation at 180 and 260 K as shown in Fig. 2, with 50% of them rotating to a new orientation, which shows the same interaction with the co-crystallized NiOEP. Both orientations are related by a mirror symmetry passing through NiOEP, as shown in Fig. S2 in the ESI.† The surprisingly different dynamic behaviours of C_{80} cages in a similar crystal lattice originate from the effects of benzene–fullerene interactions (π–π and C–H⋯π), as shown in Fig. 3, and Fig. S3 and Fig. S4 in the ESI.† The contribution of C–H⋯π is small compared to the π–π interactions,[48] while the positions of two benzene molecules interacting with the fullerene through π–π interactions show a surprisingly powerful effect on the fullerene rotation, *i.e.*, the fullerene starts rotation from 180 K when the two benzene molecules sit parallel, while the fullerene rotation is blocked until 280 K when the two benzene molecules sit with a magic angle of 125.1(8)° determined at 100 K.

The Dy_2ScN cluster shows heavy disorder at 180 and 260 K, which hampers the assignment of Dy and Sc; thus, we applied heavier Dy with free occupancies to refine the positions of Dy/Sc.[38] The positions of metal ions at 180 and 260 K show a tendency of "spinning top" rotation as observed for $M_3N@C_{80}$ (M_3 = Ho_2Lu, Lu_3).[26] The possibility of two metal ions near the NiOEP (labelled as **II** and **III** in Fig. 2) rotating to the far away position (labelled as **I**) is impossible to clarify in the case of

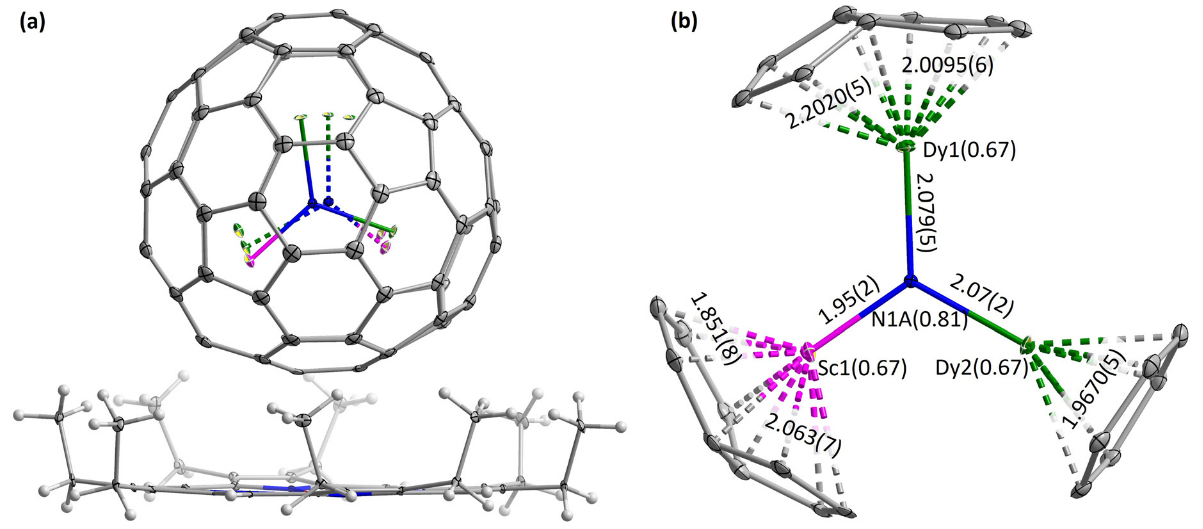

Fig. 1 The structure of $Dy_2ScN@C_{80}$·NiOEP·$2C_6H_6$ with omitted benzene molecules (a) and the structure of Dy_2ScN with coordinated fullerene cage fragments (b) observed at 100 K. The site occupancies with atom labels and bond lengths as well as the distance between metal ions and the coordinated hexagons/pentagons (in Å) are shown in the figure. Colour code: grey for C, white for H, blue for N, red for Ni, pink for Sc, and green for Dy. The thermal ellipsoids are set at 30% probability.

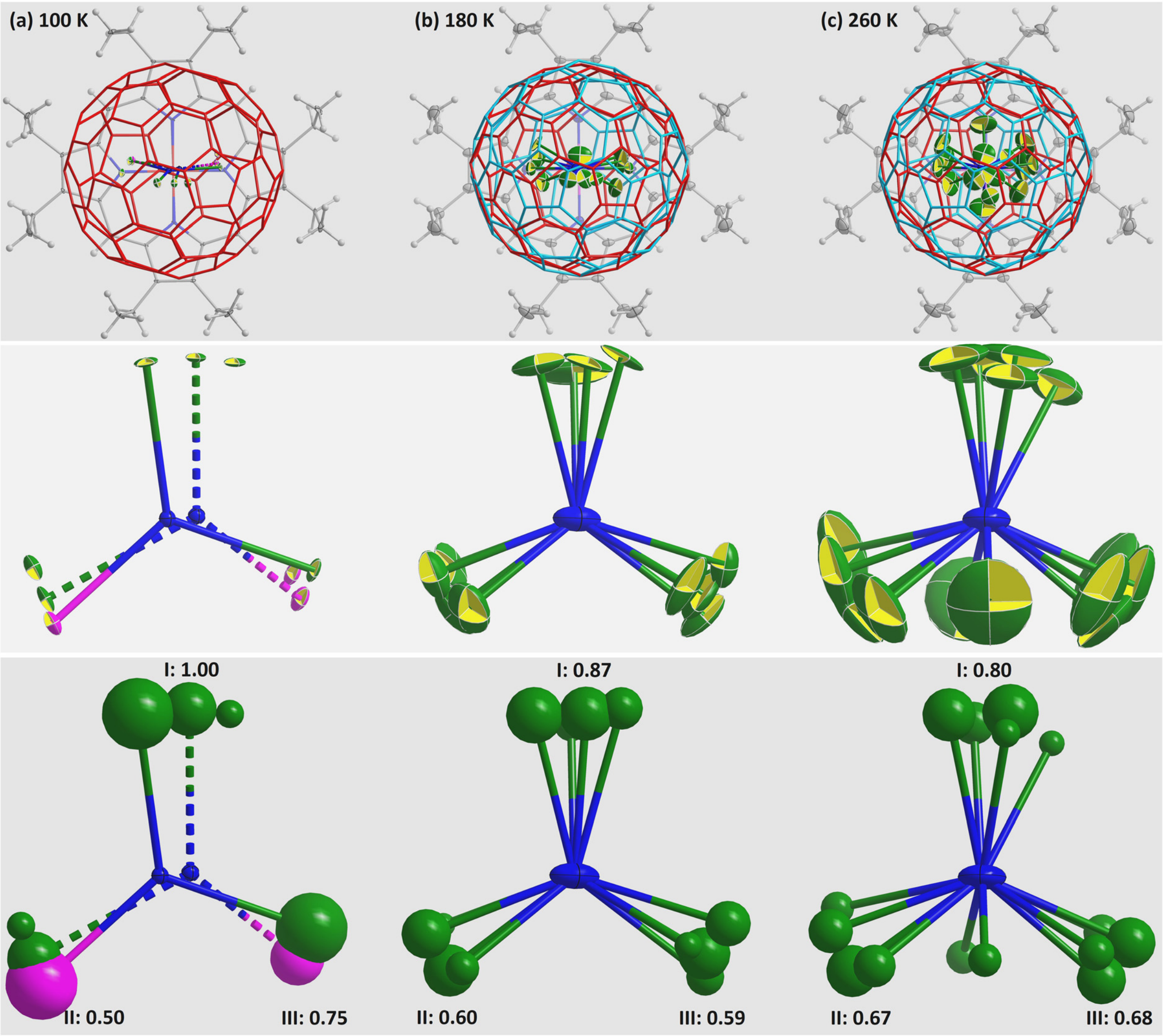

Fig. 2 The structures of $Dy_2ScN@C_{80}\cdot NiOEP\cdot 2C_6H_6$ viewed perpendicular to the NiOEP plane, observed at variable temperatures of (a) 100, (b) 180 and (c) 260 K. The structures with omitted benzene for clarity are shown in the upper panel, while the structures of the Dy_2ScN cluster are highlighted in the middle panel, and the lower panel shows the Dy_2ScN structure with a metal volume equal to the site occupancy, and the three main metal positions are labelled (**I** labels the position far away from NiOEP; **II** and **III** label the positions near the NiOEP, with the equivalent Dy occupancies noted in the figure) with their electron density gauged with equivalent Dy occupancies. Colour code: grey for C, white for H, blue for N, red for Ni, pink for Sc, and green for Dy. The thermal ellipsoids are set at 30% probability except for C_{80}. C_{80} is highlighted with red/cyan to show the orientations.

$M_3N@C_{80}$ (M_3 = Ho_2Lu, Lu_3) because of similar electron densities at the three positions (**I**, **II**, and **III**). $Dy_2ScN@C_{80}$ is ideal to clarify such a possibility with substantially different Dy and Sc electron densities (1Sc ≈ 0.25Dy in the refinement considering the effects of scattering power). The electron density imbalance of 0.50 : 0.75 (normalized with Dy) between **II** and **III** at 100 K is averaged off to 0.60 : 0.59 at 180 K, while the imbalance between **I** and **II**/**III** shows a tendency of averaging off with increasing temperature as shown in Fig. 2. Contrary to the disordered N at 100 K, the N is fully ordered at 180 and 260 K and is located at the centroid of C_{80}. Because the N is pushed out of the centroid of C_{80} by the inequivalent Dy/Sc ions (*vide supra*), it does not occupy the crystallographically ordered N position. The flattened ellipsoids of N at 180 and 260 K hint at the rotation of N around the C_{80} centroid (see Fig. S5 in the ESI† for details). Thus, the assumption that the main position represents the real structure in single crystal X-ray diffraction involving disorder should be applied with caution. It is worth noting that the structures obtained at 180 and 260 K result in misrepresented Dy_2SCN structures as shown in Table S2 in the ESI.† The Dy–N bond lengths of 2.07 (2) and 2.079(5) Å determined at 100 K change to 2.052(5) and 1.949(6) Å at 180 K and to 2.019(9) and 1.935(11) Å at 260 K, showing remarkable discrepancies.

For most $M_3N@C_{80}$ co-crystallized with NiOEP, two metal atoms of M_3N prefer to sit above the N–Ni–N bonds.[24,26,49–51]

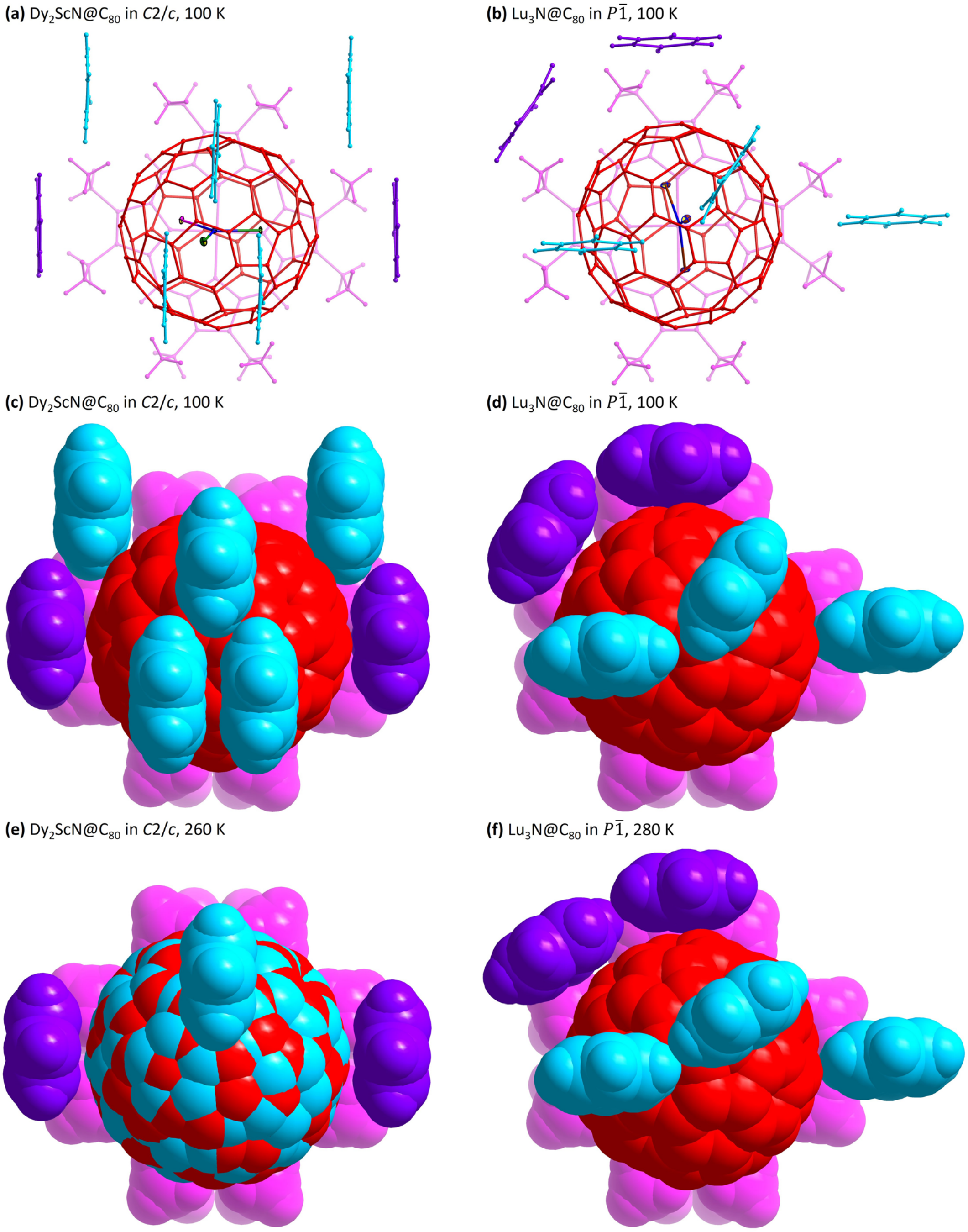

Fig. 3 The structures of $Dy_2ScN@C_{80}\cdot NiOEP\cdot 2C_6H_6$ in the $C2/c$ space group (a, c and e) and $Lu_3N@C_{80}\cdot NiOEP\cdot 2C_6H_6$ in the $P\bar{1}$ space group (b, d, f, data from ref. 26) viewed perpendicular to the NiOEP plane. The ball-stick model is shown in the upper panel, while the space-filling structures are shown in the middle/lower panels. Colour code: red/cyan for the fullerene cage, pink for NiOEP, purple for benzene interacting with the fullerene cage through π–π interactions, and cyan for benzene interacting with the fullerene cage through C–H⋯π interactions.

The recently reported $M_2@C_{80}$-CF_3 (M = Tb, Nd) co-crystallized with NiOEP also shows such tendency.[5,52] The Dy_2ScN cluster shown in Fig. S6 in the ESI† reveals that the encapsulated Dy_2ScN sits above the N–Ni–N bonds at 100 K, while exhibiting rotation at 180 and 260 K, showing the subtle interaction between metal ions and the NiOEP molecule.

In conclusion, the structure of $Dy_2ScN@C_{80}$ was determined by variable temperature single crystal X-ray diffraction. The temperature-driven dynamics of $Dy_2ScN@C_{80}$ in the lattice was precisely recorded in great detail. The angle between the two benzenes interacting with the fullerene cage through π–π interaction shows a surprising ability to control the fullerene cage rotation. These results present a deep understanding of the metallofullerene structures, facilitating their high-accuracy structure–property relationship investigation.

Author contributions

Y. W. synthesized fullerenes, Y. W. and F. L. prepared the crystals and conducted the single crystal X-ray diffraction measurement and analysis. F. L. wrote the manuscript with a contribution from Y. W.

Conflicts of interest

There are no conflicts of interest to declare.

Acknowledgements

This research was financially supported by the Deutsche Forschungsgemeinschaft (LI 3055/3-1) and the Jiangsu Specially Appointed Professorship. The authors appreciate the great support of and fruitful discussion with Dr Alexey A. Popov. Diffraction data have been collected on BL14.2 at the BESSY II electron storage ring operated by the Helmholtz-Zentrum Berlin. The authors appreciate the help of Dr Manfred Weiss and his team during the experiments at BESSY II.

References

1 A. A. Popov, S. Yang and L. Dunsch, Endohedral Fullerenes, *Chem. Rev.*, 2013, **113**, 5989–6113.

2 X. Lu, L. Feng, T. Akasaka and S. Nagase, Current status and future developments of endohedral metallofullerenes, *Chem. Soc. Rev.*, 2012, **41**, 7723–7760.

3 S. Yang, T. Wei and F. Jin, When metal clusters meet carbon cages: endohedral clusterfullerenes, *Chem. Soc. Rev.*, 2017, **46**, 5005–5058.

4 F. Liu, L. Spree, D. S. Krylov, G. Velkos, S. M. Avdoshenko and A. A. Popov, Single-Electron Lanthanide-Lanthanide Bonds Inside Fullerenes toward Robust Redox-Active Molecular Magnets, *Acc. Chem. Res.*, 2019, **52**, 2981–2993.

5 W. Yang, G. Velkos, M. Rosenkranz, S. Schiemenz, F. Liu and A. A. Popov, Nd—Nd Bond in I_h and D_{5h} Cage Isomers of $Nd_2@C_{80}$ Stabilized by Electrophilic CF_3 Addition, *Adv. Sci.*, 2024, **11**, 2305190.

6 W. Yang, M. Rosenkranz, G. Velkos, F. Ziegs, V. Dubrovin, S. Schiemenz, L. Spree, M. F. de Souza Barbosa, C. Guillemard, S. M. Valvidares, B. Büchner, F. Liu, S. Avdoshenko and A. A. Popov, Covalency versus magnetic axiality in Nd molecular magnets: Nd-photoluminescence, strong ligand-field, and unprecedented nephelauxetic effect in fullerenes $NdM_2N@C_{80}$ (M = Sc, Lu, Y), *Chem. Sci.*, 2024, **15**, 2141–2157.

7 R. Guan, J. Huang, J. Xin, M. Chen, P. Du, Q. Li, Y.-Z. Tan, S. Yang and S.-Y. Xie, A stabilization rule for metal carbido cluster bearing μ_3-carbido single-atom-ligand encapsulated in carbon cage, *Nat. Commun.*, 2024, **15**, 150.

8 P. Yu, M. Li, S. Hu, C. Pan, W. Shen, K. Guo, Y.-P. Xie, L. Bao, R. Zhang and X. Lu, Stabilizing non-IPR $C,_2$(13333)-C_{74} cage with Lu_2C_2/Lu_2O: the importance of encaged non-metallic elements, *Chem. Commun.*, 2023, **59**, 12990–12993.

9 Y.-R. Yao, J. Zhao, Q. Meng, H.-S. Hu, M. Guo, Y. Yan, J. Zhuang, S. Yang, S. Fortier, L. Echegoyen, W. H. E. Schwarz, J. Li and N. Chen, Synthesis and Characterization of U≡C Triple Bonds in Fullerene Compounds, *J. Am. Chem. Soc.*, 2023, **145**, 25440–25449.

10 Y.-R. Yao, Z.-C. Chen, L. Chen, S.-Y. Zheng, S. Yang, S.-L. Deng, L. Echegoyen, Y.-Z. Tan, S.-Y. Xie and L.-S. Zheng, Two Metastable Endohedral Metallofullerenes $Sc_2C_2@C,_1$(39656)-C_{82} and $Sc_2C_2@C_1$(51383)-C_{84}: Direct-C_2-Insertion Products from Their Most Stable Precursors, *J. Am. Chem. Soc.*, 2023, **145**, 16778–16786.

11 Y. Yan, L. Abella, R. Sun, Y.-H. Fang, Y. Roselló, Y. Shen, M. Jin, A. Rodríguez-Fortea, C. de Graaf, Q. Meng, Y.-R. Yao, L. Echegoyen, B.-W. Wang, S. Gao, J. M. Poblet and N. Chen, Actinide-lanthanide single electron metal-metal bond formed in mixed-valence di-metallofullerenes, *Nat. Commun.*, 2023, **14**, 6637.

12 W. Xiang, Z. Hu, J. Xin, H. Jin, Z. Jiang, X. Han, M. Chen, Y.-R. Yao and S. Yang, Steering Single-Electron Metal–Metal Bonds and Hyperfine Coupling between a Transition Metal-Lanthanide Heteronuclear Bimetal Confined in Carbon Cages, *J. Am. Chem. Soc.*, 2023, **145**, 22599–22608.

13 T.-X. Liu, X. Wang, S. Xia, M. Chen, M. Li, P. Yang, N. Ma, Z. Hu, S. Yang, G. Zhang and G.-W. Wang, Dearomative Ring-Fused Azafulleroids and Carbazole-Derived Metallofullerenes: Reactivity Dictated by Encapsulation in a Fullerene Cage, *Angew. Chem., Int. Ed.*, 2023, **62**, e202313074.

14 H. Jin, J. Xin, W. Xiang, Z. Jiang, X. Han, M. Chen, P. Du, Y.-R. Yao and S. Yang, Bandgap Engineering of Erbium-Metallofullerenes Toward Switchable Photoluminescence, *Adv. Mater.*, 2023, **35**, 2304121.

15 H. Jiang, X. Yu, M. Guo, Y.-R. Yao, Q. Meng, L. Echegoyen, J. Autschbach and N. Chen, USc_2C_2 and USc_2NC Clusters with U–C Triple Bond Character Stabilized Inside Fullerene Cages, *J. Am. Chem. Soc.*, 2023, **145**, 5645–5654.

16 T. Cao, Q. Meng, Z. Fu, Y. Shen, Q. Wang, Y. Yan, B. Zhao, W. Wang, K. Merimi, A. Rodriguez-Fortea, Y.-R. Yao and N. Chen, Th@$C,_2$(8)-C84 and Th@C_s(15)-C_{84}: impact of actinide metal ions on the electronic structure of actinide endohedral metallofullerenes, *Inorg. Chem. Front.*, 2023, **10**, 6901–6908.

17 P. Yu, M. Li, W. Shen, S. Hu, P.-Y. Yu, X. Tian, X. Zhao, L. Bao and X. Lu, An unprecedented C_{80} cage that violates the isolated pentagon rule, *Inorg. Chem. Front.*, 2022, **9**, 2264–2270.

18 W. Yang, G. Velkos, S. Sudarkova, B. Büchner, S. M. Avdoshenko, F. Liu, A. A. Popov and N. Chen, Carbon cage isomers and magnetic Dy⋯Dy interactions in $Dy_2O@C_{88}$ and $Dy_2C_2@C_{88}$ metallofullerenes, *Inorg. Chem. Front.*, 2022, **9**, 5805–5819.

19 W. Xiang, X. Jiang, Y.-R. Yao, J. Xin, H. Jin, R. Guan, Q. Zhang, M. Chen, S.-Y. Xie, A. A. Popov and S. Yang, Monometallic Endohedral Azafullerene, *J. Am. Chem. Soc.*, 2022, **144**, 21587–21595.

20 G. Velkos, W. Yang, Y.-R. Yao, S. M. Sudarkova, F. Liu, S. M. Avdoshenko, N. Chen and A. A. Popov, Metallofullerene single-molecule magnet $Dy_2O@C_{2v}(5)$-C_{80} with a strong antiferromagnetic Dy⋯Dy coupling, *Chem. Commun.*, 2022, **58**, 7164–7167.

21 Y. Shen, X. Yu, Q. Meng, Y.-R. Yao, J. Autschbach and N. Chen, $ThC_2@C_{82}$ versus $Th@C_{84}$: unexpected formation of triangular thorium carbide cluster inside fullerenes, *Chem. Sci.*, 2022, **13**, 12980–12986.

22 Q. Meng, L. Abella, Y.-R. Yao, D.-C. Sergentu, W. Yang, X. Liu, J. Zhuang, L. Echegoyen, J. Autschbach and N. Chen, A charged diatomic triple-bonded U≡N species trapped in C_{82} fullerene cages, *Nat. Commun.*, 2022, **13**, 7192.

23 R. Guan, Z.-C. Chen, J. Huang, H.-R. Tian, J. Xin, S.-W. Ying, M. Chen, Q. Zhang, Q. Li, S.-Y. Xie, L.-S. Zheng and S. Yang, Self-driven carbon atom implantation into fullerene embedding metal–carbon cluster, *Proc. Natl. Acad. Sci. U. S. A.*, 2022, **119**, e2202563119.

24 Y. Hao, Y. Wang, L. Spree and F. Liu, Rotation of fullerene molecules in the crystal lattice of fullerene/porphyrin: C_{60} and $Sc_3N@C_{80}$, *Inorg. Chem. Front.*, 2021, **8**, 122–126.

25 Y. Hao, Y. Wang, V. Dubrovin, S. M. Avdoshenko, A. A. Popov and F. Liu, Caught in Phase Transition: Snapshot of the Metallofullerene $Sc_3N@C_{70}$ Rotation in the Crystal, *J. Am. Chem. Soc.*, 2021, **143**, 612–616.

26 F. Liu and L. Spree, Molecular spinning top: visualizing the dynamics of $M_3N@C_{80}$ with variable temperature single crystal X-ray diffraction, *Chem. Commun.*, 2019, **55**, 13000–13003.

27 M. M. Olmstead, D. A. Costa, K. Maitra, B. C. Noll, S. L. Phillips, P. M. Van Calcar and A. L. Balch, Interaction of curved and flat molecular surfaces. The structures of crystalline compounds composed of fullerene (C_{60}, $C_{60}O$, C_{70}, and $C_{120}O$) and metal octaethylporphyrin units, *J. Am. Chem. Soc.*, 1999, **121**, 7090–7097.

28 Y.-Y. Xu, H.-R. Tian, S.-H. Li, Z.-C. Chen, Y.-R. Yao, S.-S. Wang, X. Zhang, Z.-Z. Zhu, S.-L. Deng, Q. Zhang, S. Yang, S.-Y. Xie, R.-B. Huang and L.-S. Zheng, Flexible decapyrrylcorannulene hosts, *Nat. Commun.*, 2019, **10**, 485.

29 F. Liu, G. Velkos, D. S. Krylov, L. Spree, M. Zalibera, R. Ray, N. A. Samoylova, C.-H. Chen, M. Rosenkranz, S. Schiemenz, F. Ziegs, K. Nenkov, A. Kostanyan, T. Greber, A. U. B. Wolter, M. Richter, B. Büchner, S. M. Avdoshenko and A. A. Popov, Air-stable redox-active nanomagnets with lanthanide spins radical-bridged by a metal–metal bond, *Nat. Commun.*, 2019, **10**, 571.

30 F. Liu, D. S. Krylov, L. Spree, S. M. Avdoshenko, N. A. Samoylova, M. Rosenkranz, A. Kostanyan, T. Greber, A. U. B. Wolter, B. Büchner and A. A. Popov, Single molecule magnet with an unpaired electron trapped between two lanthanide ions inside a fullerene, *Nat. Commun.*, 2017, **8**, 16098.

31 S. Stevenson, G. Rice, T. Glass, K. Harich, F. Cromer, M. R. Jordan, J. Craft, E. Hadju, R. Bible, M. M. Olmstead, K. Maitra, A. J. Fisher, A. L. Balch and H. C. Dorn, Small-bandgap endohedral metallofullerenes in high yield and purity, *Nature*, 1999, **401**, 55–57.

32 D. S. Krylov, F. Liu, A. Brandenburg, L. Spree, V. Bon, S. Kaskel, A. U. B. Wolter, B. Büchner, S. M. Avdoshenko and A. A. Popov, Magnetization relaxation in the single-ion magnet $DySc_2N@C_{80}$: quantum tunneling, magnetic dilution, and unconventional temperature dependence, *Phys. Chem. Chem. Phys.*, 2018, **20**, 11656–11672.

33 D. S. Krylov, F. Liu, S. M. Avdoshenko, L. Spree, B. Weise, A. Waske, A. U. B. Wolter, B. Büchner and A. A. Popov, Record-high thermal barrier of the relaxation of magnetization in the nitride clusterfullerene $Dy_2ScN@C_{80}$-I_h, *Chem. Commun.*, 2017, **53**, 7901–7904.

34 R. Westerström, J. Dreiser, C. Piamonteze, M. Muntwiler, S. Weyeneth, K. Krämer, S.-X. Liu, S. Decurtins, A. Popov, S. Yang, L. Dunsch and T. Greber, Tunneling, remanence, and frustration in dysprosium-based endohedral single-molecule magnets, *Phys. Rev. B: Condens. Matter Mater. Phys.*, 2014, **89**, 060406.

35 R. Westerström, J. Dreiser, C. Piamonteze, M. Muntwiler, S. Weyeneth, H. Brune, S. Rusponi, F. Nolting, A. Popov, S. Yang, L. Dunsch and T. Greber, An Endohedral Single-Molecule Magnet with Long Relaxation Times: $DySc_2N@C_{80}$, *J. Am. Chem. Soc.*, 2012, **134**, 9840–9843.

36 C. Schlesier, L. Spree, A. Kostanyan, R. Westerström, A. Brandenburg, A. Wolter, S. Yang, T. Greber and A. A. Popov, Strong carbon cage influence on the single molecule magnetism in Dy-Sc nitride clusterfullerenes, *Chem. Commun.*, 2018, **54**, 9730–9733.

37 M. Nie, J. Liang, C. Zhao, Y. Lu, J. Zhang, W. Li, C. Wang and T. Wang, Single-Molecule Magnet with Thermally Activated Delayed Fluorescence Based on a Metallofullerene Integrated by Dysprosium and Yttrium Ions, *ACS Nano*, 2021, **15**, 19080–19088.

38 Y. Hao, G. Velkos, S. Schiemenz, M. Rosenkranz, Y. Wang, B. Büchner, S. Avdoshenko, A. A. Popov and F. Liu, Using internal strain and mass to modulate Dy⋯Dy coupling and relaxation of magnetization in heterobimetallic metallofullerenes $DyM_2N@C_{80}$ and $Dy_2MN@C_{80}$ (M = Sc, Y, La, Lu), *Inorg. Chem. Front.*, 2023, **10**, 468–484.

39 M. Nie, J. Xiong, C. Zhao, H. Meng, K. Zhang, Y. Han, J. Li, B. Wang, L. Feng, C. Wang and T. Wang, Luminescent single-molecule magnet of metallofullerene $DyErScN@I_h$-C_{80}, *Nano Res.*, 2019, **12**, 1727–1731.

40 L. Spree, C. Schlesier, A. Kostanyan, R. Westerström, T. Greber, B. Büchner, S. Avdoshenko and A. A. Popov, Single molecule magnets $DyM_2N@C_{80}$ and $Dy_2MN@C_{80}$ (M = Sc, Lu): The impact of diamagnetic metals on the Dy^{3+} magnetic anisotropy, Dy⋯Dy coupling, and mixing of molecular and lattice vibrations, *Chem. – Eur. J.*, 2019, **26**, 2436–2449.

41 C. Huang, R. Sun, L. Bao, X. Tian, C. Pan, M. Li, W. Shen, K. Guo, B. Wang, X. Lu and S. Gao, A hard molecular nanomagnet from confined paramagnetic 3d-4f spins inside a fullerene cage, *Nat. Commun.*, 2023, **14**, 8443.

42 L. Spree and A. A. Popov, Recent advances in single molecule magnetism of dysprosium-metallofullerenes, *Dalton Trans.*, 2019, **48**, 2861–2871.

43 C. Schlesier, F. Liu, V. Dubrovin, L. Spree, B. Büchner, S. M. Avdoshenko and A. A. Popov, Mixed dysprosium-lanthanide nitride clusterfullerenes $DyM_2N@C_{80}$-I_h and $Dy_2MN@C_{80}$-I_h (M = Gd, Er, Tm, and Lu): synthesis, molecular structure, and quantum motion of the endohedral nitrogen atom, *Nanoscale*, 2019, **11**, 13139–13153.

44 U. Mueller, R. Förster, M. Hellmig, F. U. Huschmann, A. Kastner, P. Malecki, S. Pühringer, M. Röwer, K. Sparta, M. Steffien, M. Ühlein, P. Wilk and M. S. Weiss, The macromolecular crystallography beamlines at BESSY II of the Helmholtz-Zentrum Berlin: Current status and perspectives, *Eur. Phys. J. Plus*, 2015, **130**, 141.

45 W. Kabsch, XDS, *Acta Crystallogr., Sect. D: Biol. Crystallogr.*, 2010, **66**, 125–132.

46 K. M. Sparta, M. Krug, U. Heinemann, U. Mueller and M. S. Weiss, XDSAPP2.0, *J. Appl. Crystallogr.*, 2016, **49**, 1085–1092.

47 G. Sheldrick, Crystal structure refinement with SHELXL, *Acta Crystallogr., Sect. C: Struct. Chem.*, 2015, **71**, 3–8.

48 M.-M. Li, Y.-B. Wang, Y. Zhang and W. Wang, The Nature of the Noncovalent Interactions between Benzene and C_{60} Fullerene, *J. Phys. Chem. A*, 2016, **120**, 5766–5772.

49 S. Stevenson, C. J. Chancellor, H. M. Lee, M. M. Olmstead and A. L. Balch, Internal and external factors in the structural organization in cocrystals of the mixed-metal endohedrals ($GdSc_2N@I_h$,-C_{80}, $Gd_2ScN@I_h$-C_{80}, and $TbSc_2N@I_h$-C_{80}) and nickel(II) octaethylporphyrin, *Inorg. Chem.*, 2008, **47**, 1420–1427.

50 M. M. Olmstead, T. Zuo, H. C. Dorn, T. Li and A. L. Balch, Metal Ion Size and the Pyramidalization of Trimetallic Nitride Units Inside a Fullerene Cage: Comparisons of the Crystal Structures of $M_3N@I_h$,-C_{80} (M = Gd, Tb, Dy, Ho, Er, Tm, Lu, and Sc) and Some Mixed Metal Counterparts, *Inorg. Chim. Acta*, 2017, **468**, 321–326.

51 V. Dubrovin, L.-H. Gan, B. Büchner, A. A. Popov and S. Avdoshenko, Endohedral metal-nitride cluster ordering in metallofullerene-NiII(OEP) complexes and crystals: a theoretical study, *Phys. Chem. Chem. Phys.*, 2019, **21**, 8197–8200.

52 Y. Wang, G. Velkos, N. J. Israel, M. Rosenkranz, B. Büchner, F. Liu and A. A. Popov, Electrophilic Trifluoromethylation of Dimetallofullerene Anions en Route to Air-Stable Single-Molecule Magnets with High Blocking Temperature of Magnetization, *J. Am. Chem. Soc.*, 2021, **143**, 18139–18149.